**J. Cent. South Univ.** (2015) 22: 1287−1297
**DOI:** 10.1007/s11771-015-2645-0

Springer

# Design of relief-cavity in closed-precision forging of gears

ZUO Bin(左斌), WANG Bao-yu(王宝雨), LI Zhi(李智), ZHENG Ming-nan(郑明男), ZHU Xiao-xing(朱小星)

School of Mechanical Engineering, University of Science and Technology Beijing, Beijing 100083, China



**Abstract:** To reduce the difficulty of material filling into the top region of tooth in hot precision forging of gears using the alternative die designs, relief-cavity designs in different sizes were performed on the top of die tooth. The influences of the conventional process and relief-cavity designs on corner filling, workpiece stress, die stress, forming load and material utilization were examined. Finite element simulation for tooth forming, die stress and forming load using the four designs was performed. The material utilization was further considered, and the optimal design was determined. The tooth form and forming load in forging trials ensured the validity of FE simulation. Tooth accuracy was inspected by video measuring machine (VMM), which shows the hot forged accuracy achieves the level of rough machining of gear teeth. The effects of friction on mode of metal flow and strain distribution were also discussed.

**Key words:** gear forging; precision forging; relief-cavity; alternative die; metal flow; corner filling

## 1 Introduction

Compared to the conventional cutting gears, the forged gears have the advantages of high strength of tooth in high production efficiency, low material wastage and power dissipation [1−7]. But the difficulty in metal filling into the corner, which leads to high forging load and die distortion, has to be reduced for commercial production [8].

In the past years, researches on process designs to reduce the forming load in precision forging techniques of gears have been increasing gradually. Different structure and shape designs of tools can significantly improve the material flow so that the difficulty of corner filling is reduced. The benefits are the lower forming load and die stress, and higher accuracy. The idea of relief-axis and relief-hole based on divided flow principle was used in gear forging by OHGA et al [9] to reduce the forging load and contribute to the complete filling up by causing an inward material flow by forming a relief-axis or by shrinking the diameter of the relief-hole [9]. Alternative die design was proposed by CAI et al [10], in which the toothed die moves downwards with the punch so that the frictional force can assist the material to flow downwards to contribute to the filling on the bottom corner of tooth. They also put forward the chamfered punch to reduce the forming load [10]. A new technological scheme of dies was studied by HU et al [11], concluding that the punch end face in a waveform shape was the best scheme to better the strain distribution and secure the effective material radial flow of workpiece. The results show that the corner filling is improved and well-shaped gears are forged [11]. HU et al [12] proposed the rigid-parallel-motive (RPM) flow mode, based on which a novel specific gear forging technology was put forward by introducing upend forging process and constrained divided-flow technique. The experimental result shows that forming load is reduced by 35% compared with the conventional process. A new cold precision forging process proposed by WANG et al [13] suggested that the fabricating process of the spur gear was divided into two steps, reducing the forging load by 30% and improving filling ability of the tooth profile [13]. FENG and HUA [14] optimized the process parameters for the helical gear precision forging using finite element method and Taguchi method with multi-objective design, revealing that the most significant parameters affecting the maximum forming load and the die-fill quality are forging temperature and friction coefficient.

This work improves the aspects of hot closed-precision forging of gears based on the design alternative die and chamfered punch. Relief-cavity designs in different sizes have been performed on the top of tooth to assist the material flows in the top region of tooth. The influences of different designs on corner filling, workpiece stress, die stress, forming load and material utilization were discussed to determine the optimal design. The tooth accuracy was inspected by video

**Foundation item:** Project(51375042) supported by the National Natural Science Foundation of China; Project supported by Beijing Laboratory of Modern Transport Metal Materials and Processing Technology, China
**Received date:** 2014−02−27; **Accepted date:** 2014−07−10
**Corresponding author:** WANG Bao-yu, PhD; Tel: +86−10−62332331; E-mail: bywang@ustb.edu.cn

measuring machine (VMM), which shows the forged accuracy achieves the level of rough machining of gear teeth. At last, the effects of friction on mode of metal flow and strain distribution in forging process using the relief-cavity were studied.

## 2 Relief-cavity design based on alternative toothed die

### 2.1 Alternative toothed die design

Alternative die design was first put forward by CAI et al [10], as well as chamfered punch. In the tool design, the toothed die is attached to the machine bed by several springs while the counter punch is fixed to the machine bed, as shown in Fig. 1. When the punch presses down and kisses the toothed die, the cavity is completely closed. Then, the toothed die moves together with the punch till the billet filling up the cavity. The movable toothed die can change the direction of the frictional force downward so that the bottom corner of the tooth will be filled up before the top corner. Although the friction becomes positive for the fills of the bottom corner, the difficulty of material filling on the top corner increases. In addition, the chamfered punch can significantly reduce the forming load by 45% according to CAI et al's study.

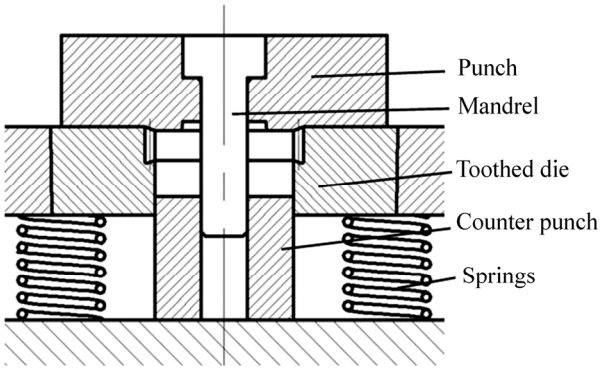


**Fig. 1** Alternative die design

### 2.2 Relief-cavity design

The gear with a module of 2.117 mm and teeth number of 31 was taken in the study for hot precision forging. The height of the gear is 17 mm and the material is AISI 8620. The billets to be forged were made into the shape of hollow cylinder with their external diameter close to the root diameter of the gear. The tool set with the structure of alternative die was used.

There are three stages in precision forging: upsetting, filling the container and filling the corner [15]. In the first two stages, the forming load increases gradually, but a significant increase arises in the last stage. The sharp corners on the tooth aggravate the difficulties of the corner filling. So, the cavity designs which have no or few sharp corners to be filled can reduce forming load and tool stress. Less die distortion and longer tool life will be emerged. In order to smooth the top corner of tooth in the tool with the structure of alternative die to ease the material filling on the top region of tooth, relief-cavity designs in different sizes on the top corner of tooth were settled on the toothed die and the punch. As Fig. 2(a) shows, the common die with no relief-cavity (namely relief-cavity thickness $a$ is zero) is chamfered on the corner of teeth to assist the corner filling, which is similar to the designs in Ref. [10]. The schematic diagram of the relief-cavity on the top corner of teeth is shown in Fig. 2(b), in which the relief-cavity thickness is illustrated. Designs with relief-cavity thickness $a$=1, 2 and 3 mm were studied in this work.

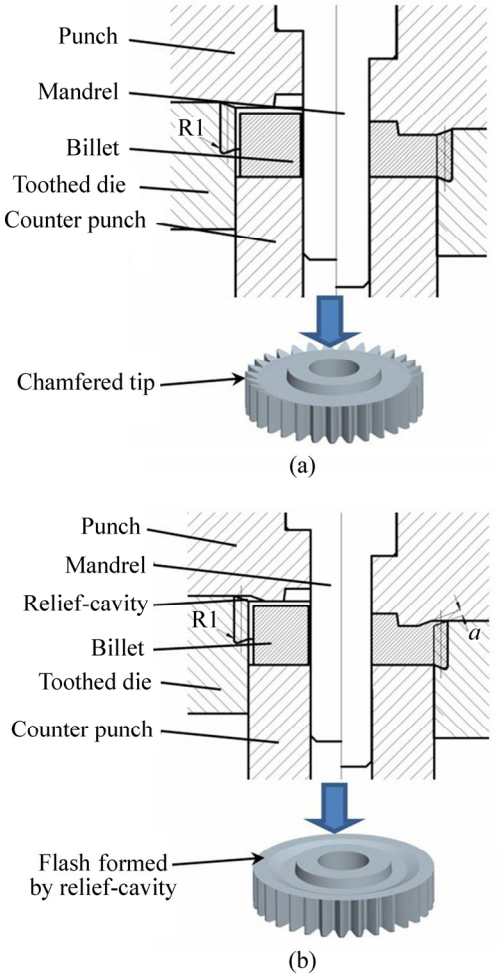


**Fig. 2** Schematic diagrams of relief-cavity designs and gears to be forged: (a) Chamfered punch with no relief-cavity (Process I); (b) Chamfered punch with relief-cavity (Process II)

## 3 FE modeling of forging process

The forging process using the two types of tool designs were analyzed with finite element method. Taking the die with no relief- cavity for example, the four parts of tools and the billet for FE model illustrated in Fig. 4 were constructed by Pro-ENGINEER for

geometry and DEFORM-3D for FE simulation, all of which were in a portion corresponding to one tooth because of the symmetry. The mandrel, punch and counter punch were modeled as rigid body at preheated temperature of 100 °C while the toothed die as elastic one for analyzing the die stress in the forging process. The billet was plastic body and heated to 1000 °C and 1000 steps were set up for simulating process.

The material of the toothed die was H13 and the billet AISI 8620 steel. The chemical composition of billet material is listed in Table 1.

**Table 1** Chemical composition of AISI 8620 alloy (mass fraction, %)

| C | Cr | Ni | S | |
|---|---|---|---|---|
| 0.18−0.23 | 0.4−0.6 | 0.4−0.7 | ≤0.040 | |
| Si | P | Mn | V | Fe |
| 0.15−0.35 | ≤0.035 | 0.7−0.9 | 0.15−0.25 | Bal. |

The elastic modulus and poisson ratio of AISI 8620 are 206.7 GPa and 0.3, respectively. The flow stress can be defined as a function determined by train, train rate and temperature:

$$\sigma = \sigma(\varepsilon, \dot{\varepsilon}, T) \tag{1}$$

where $\sigma$ is the flow stress, $\varepsilon$ is the plastic strain and $\dot{\varepsilon}$ is the plastic strain rate of the workpiece material.

The flow stress data of billet material come from the material library of software DEFORM-3D. Figure 3 shows the flow stress curves at different temperatures and train rates.

There exists friction prevailing at the die−workpiece interface at all times during the forging process. Furthermore, friction conditions have great effects on the material deformation and forming load. Therefore, accurately specifying the friction conditions for the FE simulation can result in valid prediction. Usually, the constant shear friction law is used for bulk forming simulations due to large plastic deformation. The frictional force in the constant shear model is defined in Eqs. (2) and (3). It can be explained that when the shear stress caused by friction is larger than the product of effective flow stress and friction factor, the friction will occur. In this work, a frictional factor of $f$=0.3 between the interfaces of billet and dies was used in FE simulation according to the previous researches on friction factor in hot precision forging [16−17]:

$$\tau = f\bar{\sigma} \tag{2}$$

$$f = \frac{m}{\sqrt{3}} \tag{3}$$

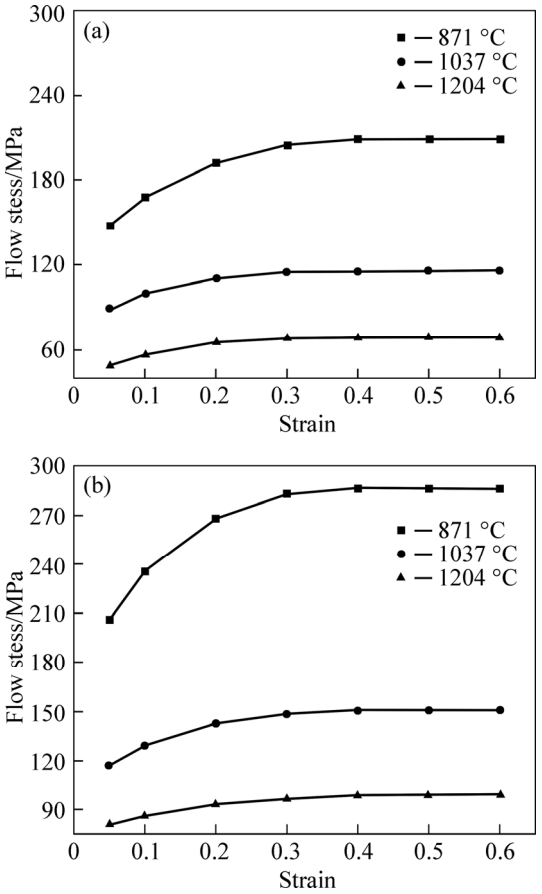


**Fig. 3** Flow stress of AISI 8620 at different strain rates: (a) 2.8 $s^{-1}$; (b) 27.5 $s^{-1}$

where $\tau$ is the frictional shear stress, $\bar{\sigma}$ is the effective flow stress of the workpiece material and $m$ ($0<m<1$) is the shear factor.

There were 30000 meshes generated on the billet and 50000 on the toothed die. For the sake of decreasing computer CPU time as well as ensuring the simulation accuracy and geometry resolution, meshes around the tooth of both billet and toothed die were locally refined with the ratio of 0.1, as shown in Fig. 4. Global remeshing method was adopted in simulation, of which

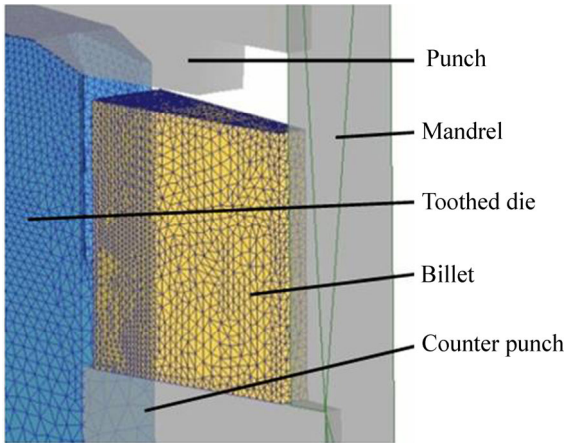


**Fig. 4** FE model for gear forging

the relative interference depth with the ratio of 0.7 was used in this work, namely, when an element edge of meshed body has been penetrated by the dies with a relative amount of 0.7 during the forging process, a new mesh is generated.

## 4 Results and discussion

### 4.1 Influence of relief-cavity on tooth forming

Figure 5 shows the three stages of tooth formation using two designs exported by FE simulation software. In the early stages before 75% punch stroke, the material flow in the middle region is faster than that in the two ends, being close to the open die upsetting. In the stages of 95% punch stroke, the forming situation in the design of relief-cavity with $a$=1 mm is similar to that of the non-relief- cavity forging, in which the billet touches the bottom corner before the top corner, because the relief-cavity is too small to assist the filling. In both designs of relief-cavity with $a$=2 and 3 mm, the filling situation on both corners remains almost consistent. The relief-cavity can lead to the material flowing toward the top corner of tooth. So, the billets touch both corners almost at the same time.

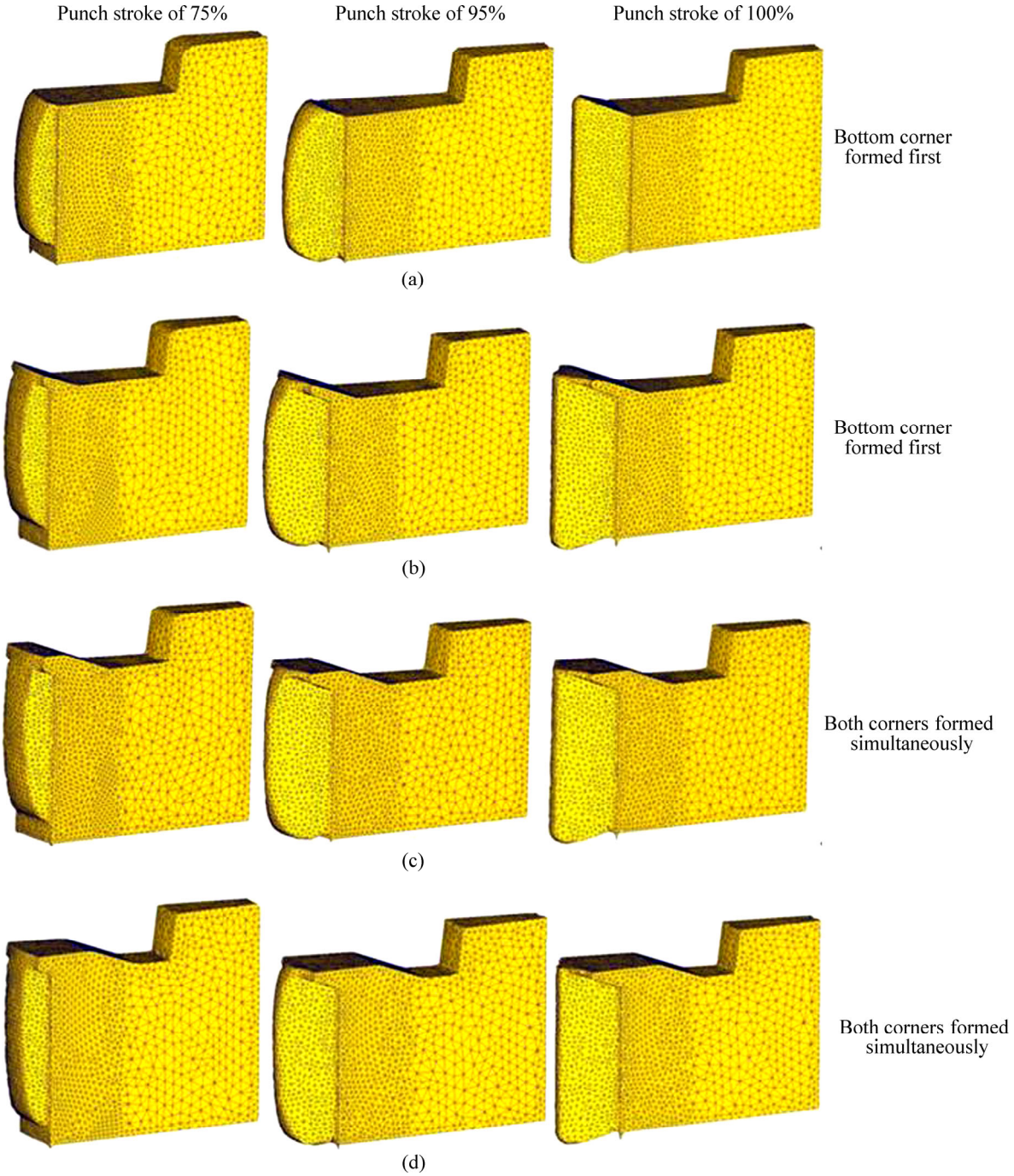


**Fig. 5** Tooth formation using two designs: (a) Process I ($a$=0); (b) Process II ($a$=1 mm); (c) Process II ($a$=2 mm); (d) Process II ($a$=3 mm)

### 4.2 Influence of relief-cavity on stress distribution in workpiece

The distributions of effective stress on the workpiece at 100% punch stroke during the precision forging process, as well as the histogram of the distribution uniformity, are shown in Fig. 6. The average effective stress, $\sigma_{avg}$, and effective stress uniformity, $\sigma_{sd}$, are define as

$$\sigma_{avg}=\sum_{i=1}^{N}\sigma_i / N \tag{4}$$

$$\sigma_{sd}=\sqrt{\sum_{i=1}^{N}\left(\sigma_i-\sigma_{avg}\right)^2 / N} \tag{5}$$

where $\sigma_i$ is the effective stress at element $i$ and $N$ is the number of elements of the gear model. Average effective stress indicates the general stress level of the workpiece, while the effective stress uniformity indicates the homogeneity of effective stress distribution. The larger value of $\sigma_{sd}$ means the less homogeneous stress distribution.

The maximum effective stress of Process I (Fig. 6(a)) locates on the addendum of the tooth and the top of the flange, as large as 370 MPa. The average effective stress $\sigma_{avg}$ is 224 MPa and the effective stress uniformity is 38.1.

When relief-cavity is designed in the forging tools, the stress level will be reduced and the uniformity will increase. In Process II ($a$=1 mm, Fig. 6(b)), the metal flows into the narrow space of relief-cavity and the addendum of tooth, so the maximum effective stress locates on the flash and the addendum, as large as 307 MPa, being 17.0% less than that in Process I. The average effective stress is 19.2% less and the effective stress distribution is 27.3% more homogeneous than that in Process I, respectively. In Process II ($a$=2 mm, Fig. 6(c)), the maximum effective stress also locates on the flash and the addendum, being 21.9% less than that in Process I. The average effective stress is 18.3% less and the effective stress distribution is 28.9% more homogeneous than that in Process I, respectively. In Process II ($a$=3 mm, Fig. 6(d)), the maximum effective stress also locates on the flash and the addendum, being 23.8% less than that in Process I. The average effective stress is 23.2% less and the effective stress distribution is 28.1% more homogeneous than that in Process I, respectively. From the histogram of effective stress distribution, the increasing size of relief-cavity results in stress distribution closer to the average stress.

To sum up the above comparisons, relief-cavity can reduce the stress level and increase the homogeneity effectively. With increasing the relief-cavity size, the maximum effective stress can be decreased but average effective stress and the effective stress uniformity remain

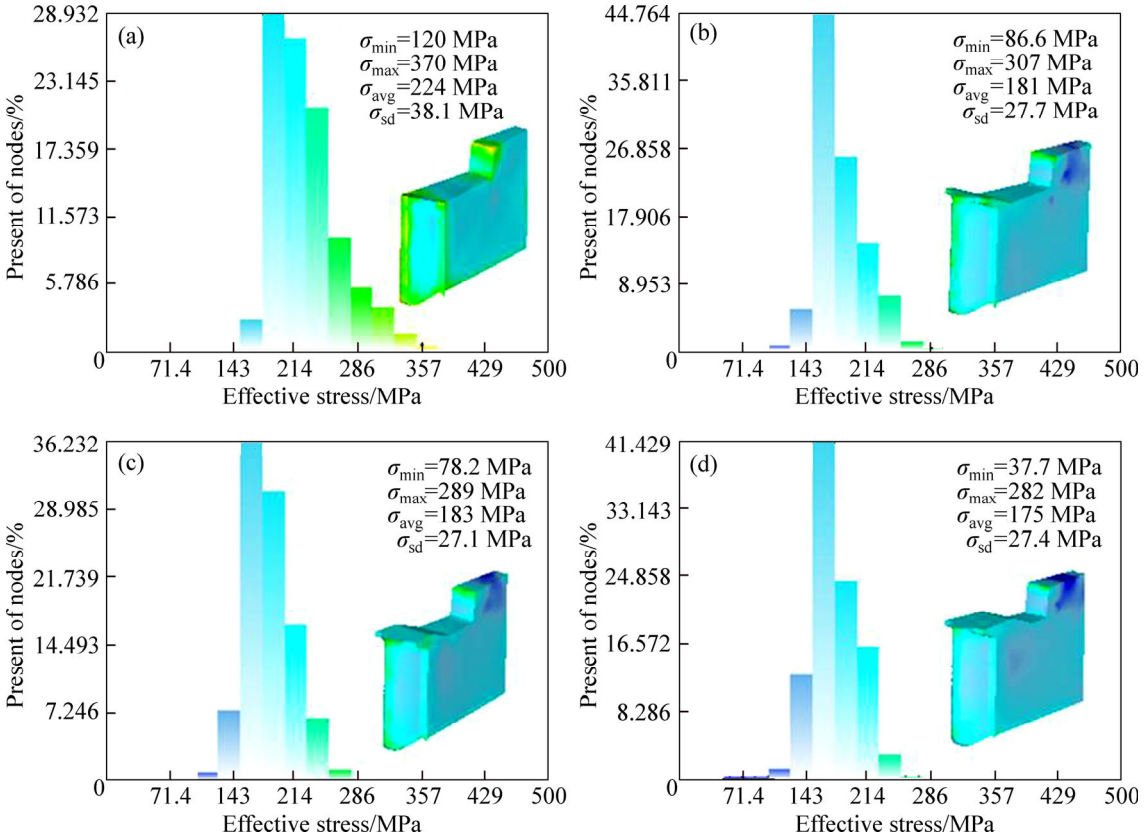


**Fig. 6** Effective stress distributions on workpiece at 100% punch stroke: (a) Process I ($a$=0); (b) Process II ($a$=1 mm); (c) Process II ($a$=2 mm); (d) Process II ($a$=3 mm)

stable, because the relief-cavity is too small, compared to the whole die cavity, to influence the global stress level and distribution.

### 4.3 Influence of relief-cavity on stress distribution on toothed die

In the final stage of gear forging, the metal fills up every corner of the cavity. The toothed die is under a considerable stress exerted by the billet. Whether the die design can significantly reduce the stress on the toothed die becomes an evaluation criterion. Lower stresses on the die mean less distortion and longer life of the tool set.

Forging with relief-cavity for gears can smooth the sharp corner to reduce the die stress. Figure 7 shows the radial stresses on the toothed die. It can be seen that the die tooth is mainly under a compressive stress, which is the main factor of plastic deformation of die tooth. The maximum stress on the die of non-relief- cavity design in the middle region of the tooth is 1560 MPa. The stress states on the die in Process II with $a$=1 mm can reduce the stress on tooth to 1470 MPa, being 5.7% less than that in Process I. The stress on die tooth in Process II with $a$=2 mm is 1420 MPa, being 8.9% less than that in Process I. Design in Process II with $a$=3 mm can significantly reduce the stress on tooth to 1350 MPa, being 13.5% less than that in Process I.

Figure 8 shows the circumferential stresses on the toothed die. It can be seen that the die tooth is under a compressive stress while the addendum is under a tensile stress concentration. This tensile stress may lead to die cracking when it is excessive. The compressive stress on the die of non-relief-cavity design in the middle region of the tooth has the value of 1380 MPa. The tensile stress concentration appears on the addendum, as large as 1630 MPa. The compressive stress on the die tooth in Process II with $a$=1 mm is 1270 MPa, while the tensile stress concentration on the addendum is about 1510 MPa, being 7.9% and 7.3% less than Process I, respectively. Process II with $a$=2 mm can reduce the compressive stress on tooth to 1230 MPa and tensile stress concentration on the addendum to 1500 MPa, being 10.8% and 7.9% less than those in Process I, separately. Process II with $a$=3 mm can significantly reduce the compressive stress on tooth to 1160 MPa and the tensile stress concentration on the addendum to 1460 MPa, being 13.5% and 10.4% less than those in Process I,

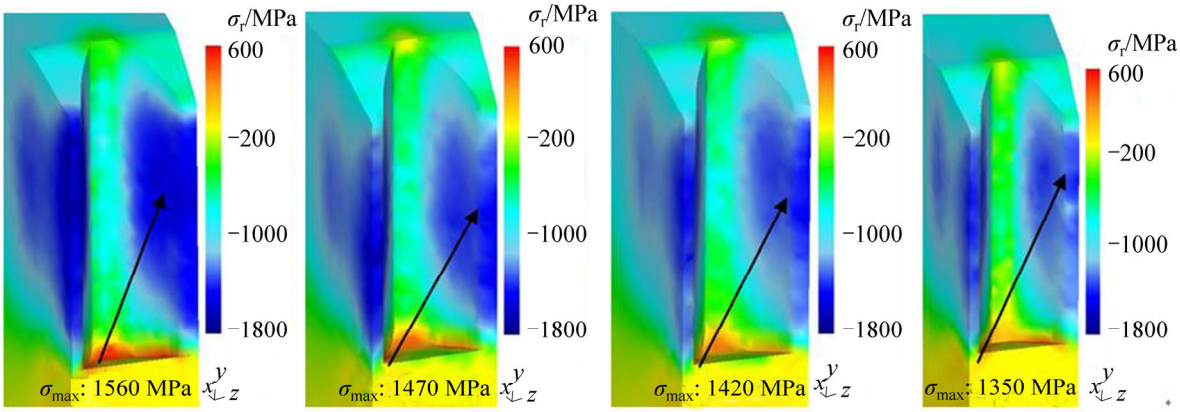


**Fig. 7** Radial stress distributions on toothed die at 100% punch stroke: (a) Process I ($a$=0); (b) Process II ($a$=1 mm); (c) Process II ($a$=2 mm); (d) Process II ($a$=3 mm)

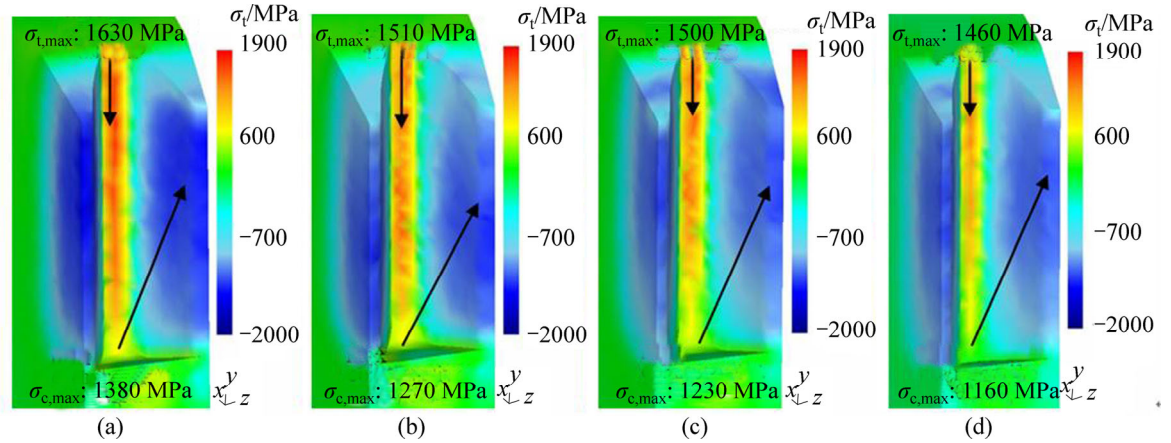


**Fig. 8** Circumferential stress distributions on toothed die at 100% punch stroke: (a) Process I ($a$=0); (b) Process II ($a$=1 mm); (c) Process II ($a$=2 mm); (d) Process II ($a$=3 mm)

respectively. It can be figured out that the bigger the relief-cavity exists, the lower the die stress requires.

### 4.4 Influence of relief-cavity on forming load

The forming loads in the forging using the two die designs in different dimensions are shown in Fig. 9. The punch strokes are different as the volumes of the billets are not the same. Forging in Process I requires the highest load as large as 4563 kN. Designs in process II with $a$=1 and 2 mm reduce the load to 4187 and 3982 kN, being 8.2% and 12.7% lower than that in Process I, respectively. Forging in Process II with $a$=3 mm requires the lowest load of 3710 kN and it is 18.7% lower than that in process I. It can be figured out that the bigger the relief-cavity exists, the lower the forming load requires.

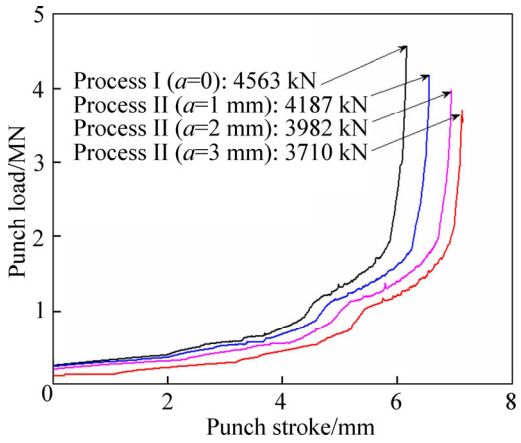


**Fig. 9** Forming loads using different die designs in FE simulation

### 4.5 Influence of friction factor on tooth forming using relief-cavity design

It is well-known that friction conditions prevailing at the die−workpiece interface have great effect on tooth formation. With the design of relief-cavity, the situation of tooth formation is changed. So, the influence of friction condition on deformation rules of metal plastic forming will be different. As larger friction force causes greater limitation of material flow and larger strain on the interfaces between the die and workpiece, strain distributions and the tooth formations are the vital foundations of research on the deformation rules of metal plastic forming. The strain distribution as well as tooth formations at the final forming stages using the relief-cavity design with thickness $a$=2 mm is shown Fig. 10, where frictional factors of $f$=0.1, 0.3 and 0.5 are employed for FE simulations.

It can be seen from Fig. 10(a) that when a low friction ($f$=0.1) exists on the interface, the top region of tooth is filled up before the bottom region. The reason is that, first, the friction between the interfaces of workpiece and moving toothed die cannot provide enough force to assist the material flowing downwards to the bottom region of the tooth. In addition, the low friction between top die and workpiece reduces the difficulty of the material on the top region of the billet flowing into the die tooth. At last, the bottom corner of the die tooth limits the material flow into the tooth corner in some degree, which is similar to the guide type forging [18]. The strain on the workpiece surface is mainly caused by the frictional shear train. So, the effective strain on the workpiece surface can demonstrate the effect of the frictional force exerting on the workpiece by the dies. The effective strain distributions show that the tooth profile around the root belongs to the largest deformation area, of which the maximum effective strain on the tooth surface is 2.74 when the friction factor is 0.1. With increasing the friction factor, the material tends to fill the bottom region of tooth much more. When the friction factor is 0.3, both corners of tooth are filled up at the same time, the same situation with the forging tests. The maximum effective strain is 3.46. When the friction factor is up to 0.5, the friction force is large enough to lead to the material filling the bottom region prior to the top corner, even there exists the relief-cavity on the top of the tooth. The maximum effective strain on the tooth profile is 4.95. Furthermore, there exists effective strain of 2.35 on the top surface of the tooth since the friction force between the top die and the workpiece limits the material flow into the top corner and causes shear strain.

From the above analysis, it is concluded that with the increase of the friction factor, the resistance of material flow into the top corner of die tooth will be enlarged and moving toothed die will lead to the material flowing into the bottom corner. The difficulty of metal flow on the workpiece surface will increase, so that the effective strain will increase. Therefore, in the precision forging process of gears, effectively reducing the friction factor will benefit the material flow and tooth forming.

### 4.6 Discussion

By comparing the several designs, they have their own advantages and disadvantages. Table 2 lists the comparison in filling situation, forming load and material utilization in the forging process using four designs. The non-relief-cavity forging requires the largest forming load among the four designs, but its material utilization is the highest. In the process of forging with relief-cavity, the relief-cavity is bigger, which means that the forming load is lower but the material waste is more. The design of Process II with $a$=3 mm requires the lowest load of 3710 kN but produces the most wastes of 12.3% of billet (volume fraction). It also reduces the resistance of material flowing into top corner so that the top corner is fully filled as bottom corner at the same time. Process II

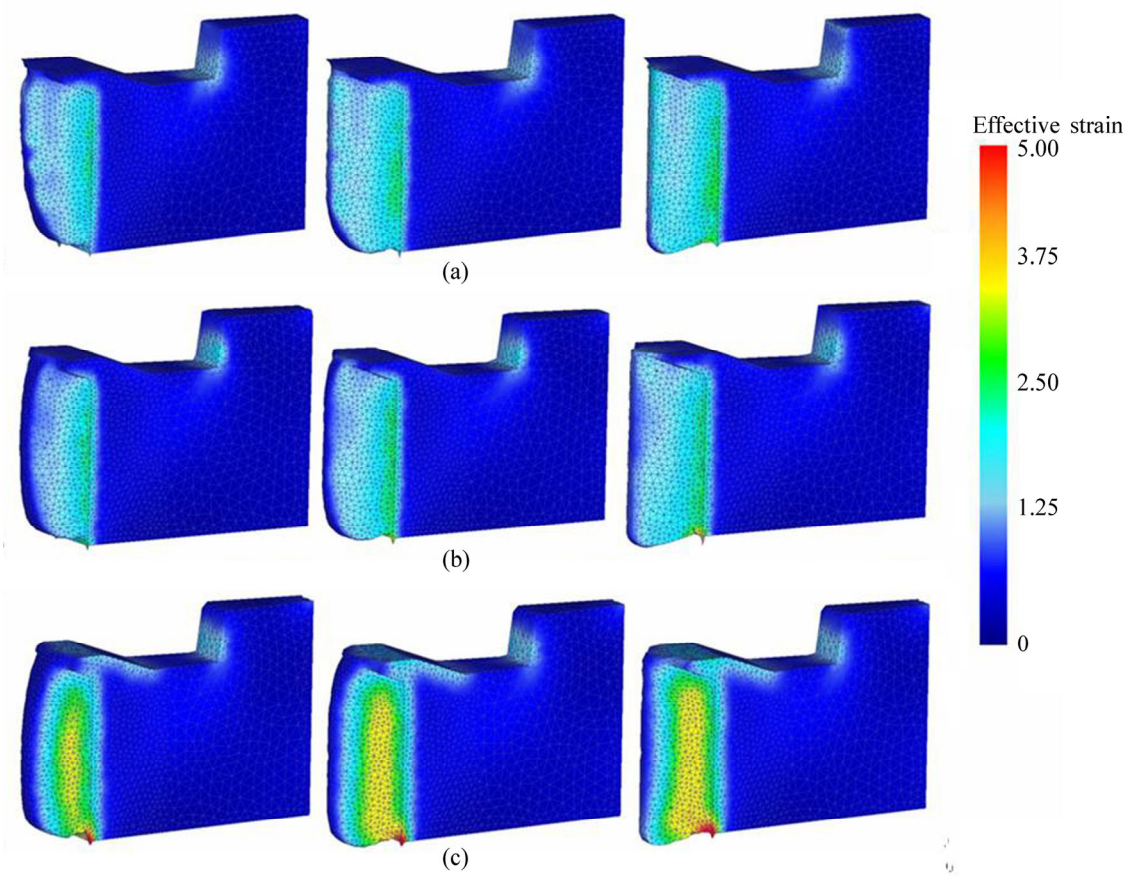


**Fig. 10** Effects of friction on effective strain and tooth forming: (a) $f$=0.1; (b) $f$=0.3; (c) $f$=0.5

**Table 2** Comparison among different relief-cavity designs

| Process | First filled region | Forming load/kN | Material utilization/% |
|---|---|---|---|
| I ($a$=0) | Bottom corner | 4563 | 94.5 |
| II ($a$=1 mm) | Bottom corner | 4187 | 92.1 |
| II ($a$=2 mm) | Top and bottom corners | 3982 | 90.0 |
| II ($a$=3 mm) | Top and bottom corners | 3710 | 87.7 |

with $a$=1 mm cannot assist the material to flow into the top corner as the relief-cavity is too small. Under the effect of the relief-cavity with $a$=2 mm, both corners are filled up at the same time. The forming load it requires is 12.7% lower than that of Process I and its material utilization is up to 90%. So, the design of process II with $a$=2 mm is recommended in this work.

## 5 Experimentation

### 5.1 Forging trials

The tool set for the design of Process I was made. After the forging trials of Process I, the dies were turned into the shape of the designs of Process II ($a$=2 mm). Forging trials using the designs in other dimension have not been done according to the previous analysis. The gear forging trials were performed on a 10 MN screw press.

Figure 11 shows the top part and the bottom part of the tool set. Material of H13 was used for the punch, mandrel, toothed die and counter punch, all of which were hardened over HRC50. The billet, made of AISI 8620, was machined in a body of a hollow cylinder. Water based graphite was used as the lubricants for the billets and dies. The gears were forged with the billets heated to 1000 °C. The tools were preheated to 100 °C to prevent the die cracking and to reduce cooling the billets. The heating time for billets was 10 min to minimize the oxidation. The two forming stages of the gear in both forging trails and FE simulations are shown in Figs. 12 and 13. The similarity of the metal flow is apparent. The tooth form was formed from the bottom to the top when forging in Process I. While the relief-cavity in Process II ($a$=2 mm) assisted the material filling on top region so that the tooth on both top and bottom region were formed together.

A load cell was installed on the punch to record the forming loads. Figure 14 shows a comparison of the forming loads between experimental measurements and FE prediction. The measured load in Process II ($a$=2 mm) is 9.7% less than that in Process I. The forming load from the FE prediction and forging trials shows close agreement with the deviation less than 9.2%.

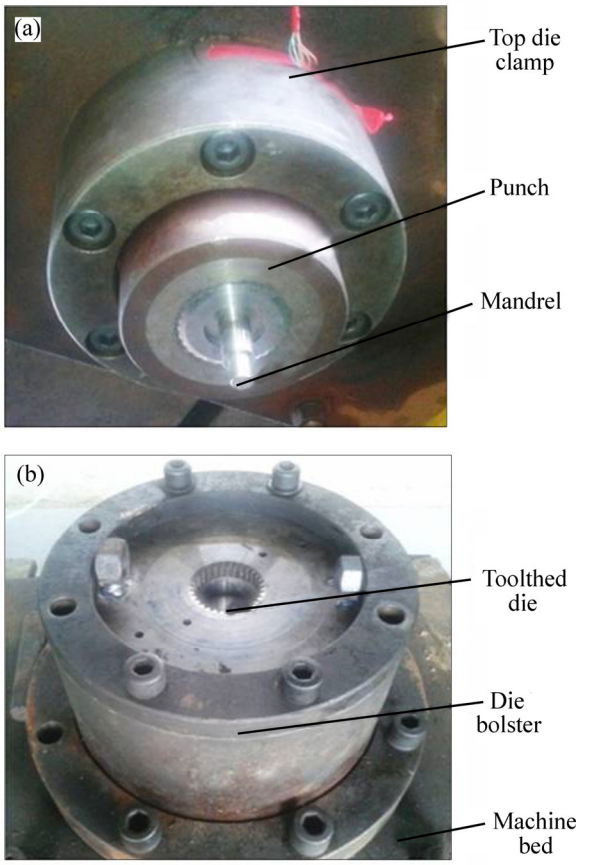


**Fig. 11** Gear forging tool set: (a) Top part; (b) Bottom part

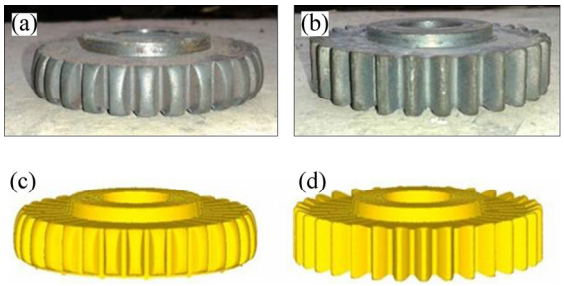


**Fig. 12** Tooth formation in gear forging Process I ($a$=0): (a) Forging trial, 85% punch stroke; (b) Forging trail, 100% punch stroke; (c) FE prediction, 85% punch stroke; (d) FE prediction, 100% punch stroke

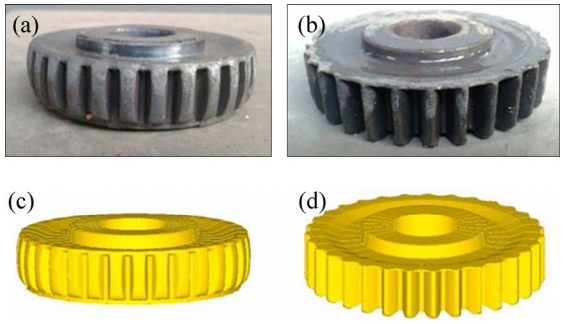


**Fig. 13** Tooth formation in gear forging Process II ($a$=2 mm): (a) Forging trial, 85% punch stroke; (b) Forging trail, 100% punch stroke; (c) FE prediction, 85% punch stroke; (d) FE prediction, 100% punch stroke

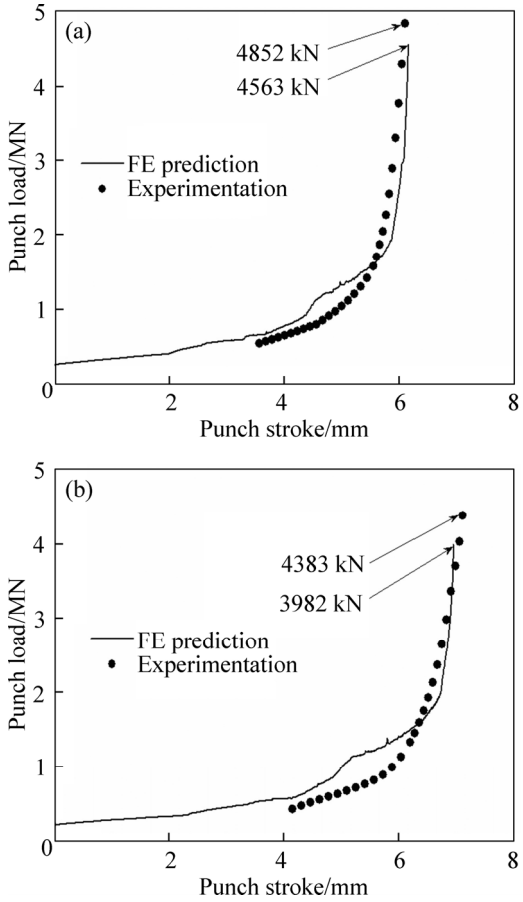


**Fig. 14** Comparison of forming loads between FE prediction and experimentation: (a) Process I ($a$=0); (b) Process II ($a$= 2 mm)

### 5.2 Tooth accuracy inspection

In the process of hot precision forging, there are several factors influencing the tooth accuracy of forged gears, such as thermal contraction and elastic recovery of workpiece, thermal expansion and elastic expansion of die. The tooth accuracy of the hot forged gears affects the following finishing process. For hot forging, thermal contraction of workpiece is the main factor of dimension variation due to the elevated forging temperature [19]. So, the tooth of the die needs to be manufactured oversize compared to the objective tooth. In the forging tests, the tooth of the die was 0.15 mm oversize in circumferential direction compared to the objective tooth and the amount was uniform along the involute profile. After forging tests, the tooth accuracy was inspected by a video measuring machine (VMM). The end faces of the forged gears were turned and the teeth were deburred so that they can be inspected. The high-resolution images of the forged gear teeth were taken by VMM. The data from the machine were processed using software Getdata Graph Digitizer and Auto CAD. Figure 15 shows the VMM and inspected tooth error.

Figure 15(b) illustrates the inspection of tooth error

(dimension difference between forged tooth and objective tooth) along the involute profile. The positive values of tooth error describe that the forged tooth is larger than the objective one. The tooth error on involute profile from the root to the addendum has the tendency of gradual decrease from 0.07 to 0.02 mm. Therefore, the dimension error of the hot forged gears in the tests is less than 0.07 mm, which achieves the accuracy level of rough machining of gear teeth.

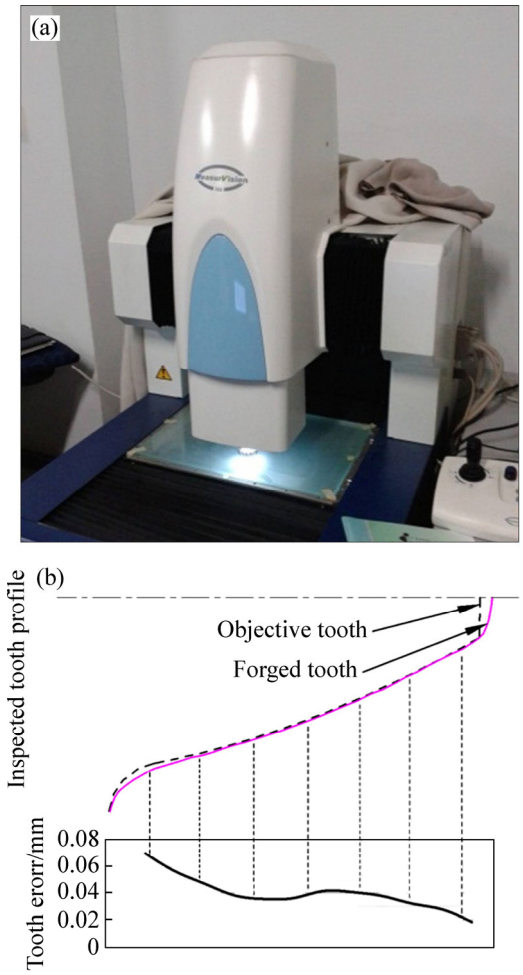


**Fig. 15** Tooth inspection: (a) Inspection equipment; (b) Inspected tooth profile and tooth erorr

## 6 Conclusions

1) The relief-cavity in different sizes can reduce the resistance of material flows in different extents. With the increase of the size of the relief-cavity, the tendency of material flowing towards the top corner of the tooth becomes evident. Too small relief-cavity cannot effectively assist the material flowing into the top corner of die tooth.

2) Relief-cavity can smooth the sharp corners and reduce the workpiece stress, die stress and forming load to different extents. The relief-cavity designs reduce the workpiece stress by about 25%. In addition, the relief-cavity designs in three sizes reduce the die stress by 6%−14% and the forming load by 8.2%−18.7%, respectively. The larger relief-cavity causes smaller die stress and forming load.

3) Further considering the material utilization in the forging process, the volume of relief-cavity is the key point. Too small volume cannot assist the material flowing or decrease the forming load effectively. Too large volume leads to much material wastes. Therefore, the relief-cavity with thickness $a$=2 mm is recommended.

4) Forging trials are performed in the tool sets using the designs of non-relief-cavity and relief-cavity with $a$=2 mm. Both the formation of tooth form and measured load verify the accuracy of the simulation. The tooth dimension error of the hot forged gears in the tests is less than 0.07 mm, which achieves the level of rough machining of gear teeth.

5) With increasing the friction factor, the situation of full filling in the bottom corner prior to top corner is evident and the effective strain on the workpiece surface increases. Therefore, effectively reducing the friction factor benefits the material flowing and tooth forming.

## References

[1] GRONOSTAJSKI Z, HAWRYLUK M. The main aspects of precision forging [J]. Archives of Civil and Mechanical Engineering, 2008, 8(2): 39−55.

[2] BEHRENS B A, DOEGE E, REINSCH S, TELKAMP K, DAEHNDEL H, SPECKER A. Precision forging processes for high-duty automotive components [J]. Journal of Materials Processing Technology, 2007, 185(1): 139−146.

[3] DEAN T A. The net-shape forming of gears [J]. Materials & Design, 2000, 21(4): 271−278..

[4] JEONG M S, LEE S K, YUN J H, SUNG J H, KIM D H, LEE S, CHOI T H. Green manufacturing process for helical pinion gear using cold extrusion process [J]. International Journal of Precision Engineering and Manufacturing, 2013, 14(6): 1007−1011.

[5] CHOI J C, CHOI Y. Precision forging of spur gears with inside relief [J]. International Journal of Machine Tools and Manufacture, 1999, 39(10): 1575−1588.

[6] SKUNCA M, SKAKUN P, KERAN Z, SIDJANIN L, MATH M D. Relations between numerical simulation and experiment in closed die forging of a gear [J]. Journal of Materials Processing Technology, 2006, 177(1): 256−260.

[7] BEHRENS B A, ODENING D. Process and tool design for precision forging of geared components [J]. International Journal of Material Forming, 2009, 2(1): 125−128.

[8] FENG Wei, HUA Lin, HAN Xing-hui. Finite element analysis and simulation for cold precision forging of a helical gear [J]. Journal of Central South University, 2012, 19: 3369−3377.

[9] OHGA K, KONDO K, JITSUNARI T. Research on precision die forging utilizing divided flow: Second report: Experimental study of processes utilizing flow relief-axis and relief-hole [J]. Bulletin of JSME, 1982, 25(209): 1836−1842.

[10] CAI J, DEAN T A, HU Z M. Alternative die designs in net-shape forging of gears [J]. Journal of Materials Processing Technology, 2004, 150(1): 48−55.

[11] HU Cheng-liang, WANG Ke-sheng, LIU Quan-kun. Study on a new technological scheme for cold forging of spur gears [J]. Journal of Materials Processing Technology, 2007, 187: 600−603.

[12] HU Cheng-liang, LIU Quan-kun, LIU Yong-xi, WANG Qiang. Analysis of metal flow and technology improvement on gear forging [J]. Chinese Journal of Mechanical Engineering, 2008, 44(5): 186−190. (in Chinese)

[13] WANG Guang-chun, ZHAO Guo-qun, XIA Shi-sheng, LUAN Yi-guo. Numerical and experimental study on new cold precision forging technique of spur gears [J]. Transactions of Nonferrous Metals Society of China, 2003, 13(4): 798−802.

[14] FENG Wei, HUA Lin. Multi-objective optimization of process parameters for the helical gear precision forging by using Taguchi method [J]. Journal of Mechanical Science and Technology, 2011, 25(6): 1519−1527.

[15] XIAO Jing-rong. Precision forging [M]. Beijing: Machine Press, 1985: 220−221. (in Chinese)

[16] SADEGH M H. Gear forging: Mathematical modeling and experimental validation [J]. Journal of Manufacturing Science and Engineering, 2003, 125(4): 753−762.

[17] YILMAZ N F, EYERCIOGLU O. An integrated computer-aided decision support system for die stresses and dimensional accuracy of precision forging dies [J]. The International Journal of Advanced Manufacturing Technology, 2009, 40(9/10): 875−886.

[18] CHOI J C, CHOI Y. A study on the forging of external spur gears: Upper-bound analyses and experiments [J]. International Journal of Machine Tools and Manufacture, 1998, 38(10/11): 1193−1208.

[19] SADEGHI M H, DEAN T A. Analysis of dimensional accuracy of precision forged axisymmetric components [J]. Proceedings of the Institution of Mechanical Engineers, Part B: Journal of Engineering Manufacture, 1991, 205(3): 171−178.

**(Edited by FANG Jing-hua)**